Supporting Information

Molecular Electrocatalysis for Oxygen Reduction by Cobalt Porphyrins Adsorbed at Liquid/Liquid Interfaces

Bin Su,[1,a] Imren Hatay,[1,4] Antonín Trojánek,[2] Zdenek Samec,[2] Tony Khoury,[3] Claude P. Gros,[3] Jean-Michel Barbe,[3] Antoine Daina,[5] Pierre-Alain Carrupt[5] and Hubert H. Girault[1,]*

[1] Laboratoire d'Electrochimie Physique et Analytique, Ecole Polytechnique Fédérale de Lausanne, Station 6, CH-1015 Lausanne, Switzerland

[2] J. Heyrovsky Institute of Physical Chemistry of ASCR, v.v.i, Dolejskova 3, 182 23 Prague 8, Czech Republic

[3] Institut de Chimie Moléculaire de l'Université de Bourgogne, ICMUB (UMR 5260), BR 47870, 21078 Dijon Cedex, France

[4] Department of Chemistry, Selcuk University, 42031 Konya, Turkey

[5] Groupe de pharmacochimie, Section des Sciences Pharmaceutiques, Quai Ernest-Ansermet 30, CH-1211 Genève 4, Switzerland

[a] Present Address: Institute of Microanalytical Systems, Department of Chemistry, Zhejiang University, Hangzhou 310058, China

*To whom correspondence should be addressed:

Fax: (+)41 21 6933667

E-mail: hubert.girault@epfl.ch

1. Porphyrin Synthesis

1.1. Instrumentation

^{1}H NMR spectra were recorded on a Bruker DRX-300 AVANCE spectrometer of the "Plateforme d'analyse chimique et de synthèse moléculaire de l'Université de Bourgogne (PACSMUB)"; chemical shifts are expressed in ppm relative to chloroform (7.258 ppm). Mass spectra were obtained on a Bruker Daltonics Ultraflex II spectrometer of the PACSMUB in the MALDI/TOF reflectron mode using dithranol as a matrix. Accurate mass measurements (HR-MS) were carried out on a Bruker MicroQTofQ instrument in ESI mode. Both measurements were made at the Centre de Spectrométrie Moléculaire de l'Université de Bourgogne. UV-visible spectra were recorded on a Varian Cary 1 spectrophotometer.

1.2. Chemicals and Reagents

All chemicals and reagents were used as received. Silica gel (Merck; 70-120 mm) was used for column chromatography. Analytical thin layer chromatography was performed using Merck 60 F_{254} silica gel (precoated sheets, 0.2 mm thick). Reactions were monitored by thin-layer chromatography and UV-visible spectroscopy.
The precursor, a,c-biladien, was synthesized as previously reported [1].

1.3. CoAP were prepared as follows (Scheme S1)

(1) 1,19-dideoxy-3,8,12,17-tetraethyl-2,7,13,18-tetramethylbiladien-a,c dibromide.
In a three-neck round bottom flask (250 mL), 3,3'-diethyl-5,5'-diformyl-4,4'-dimethyl-dipyrrylmethane [1] (2.0 g, 6.98 mmol) and 2-carboxy-3-ethyl-4-methyl-pyrrole [2, 3] (2.30 g, 15.0 mmol) synthesized according previously reported procedures, were mixed in degassed ethanol (100 mL), and the mixture was heated at reflux for 10 min. Hydrobromic acid/acetic acid solution (10 mL) was added to the reaction mixture, which was checked by UV-visible spectroscopy, the reaction was stopped after 5 min (the reaction should be stopped as quickly as possible and no more than 10 min, risking cyclisation as decomposition). The reaction mixture was cooled using an ice bath, then added to cold diethyl ether (-20 ^{o}C, 300 mL), and followed by filtration in a sintered

funnel and washing with cold ether. After drying in a desiccator, 1,19-dideoxy-3,8,12,17-tetraethyl-2,7,13,18-tetramethylbiladien-a,c dibromide (3.295 g, 75%) was obtained. UV-visible λ_{max} (CH_2Cl_2): 380 (0.567), 450 (1.397), 520 (2.81) nm.

(2) 2,8,13,17-tetraethyl-3,7,12,18-tetramethyl-5-p-nitro-phenylporphyrin.

A toluene solution (0.6 L) of *p*-toluenesulfonic acid hydrate (200 mg, 1.051 mmol) was heated at reflux for 1 h in a three-neck round bottom flask (1 L) fitted with a Dean-Stark trap and condenser, and nitrogen was bubbled through the system. *p*-Nitro-benzaldehyde (0.52 g, 3.43 mmol) and 1,19-dideoxy-3,8,12,17-tetraethyl-2,7,13,18-tetramethylbiladien-a,c dibromide (1.09 g, 1.729 mmol) were added one after another, and the addition was facilitated by using 20 ml toluene. After 1.5 h of heating, 2,3,5,6-tetrachloro-1,4-benzoquinone (1.5 g, 6.10 mmol) dissolved in toluene (25 mL) was added, and the mixture was heated for 1 h. Allowed to cool, the solvent was removed and the mixture was purified by column chromatography over silica (dichloromethane). The first purple band was collected and the solvent was removed to afford 2,8,13,17-tetraethyl-3,7,12,18-tetramethyl-5-*p*-nitro-phenylporphyrin (0.469 g, 45%) as a purple microcrystalline solid. An analytically pure sample was obtained by recrystallisation from a chloroform/methanol solution. ν_{max} (CH_2Cl_2): 3379 (NH), 1522 (NO_2), 1329 (NO_2) cm^{-1}. UV-visible λ_{max} (CH_2Cl_2) (log ε): 380 (4.98), 402 (5.19), 503 (4.13), 536 (3.81), 572 (3.77), 625 (3.40) nm. ^{1}H NMR (300 MHz, $CDCl_3$): δ -3.28, -3.23, -3.17 and -3.10 (2 H, inner NH); 1.14 (6 H, t, *J* 7.5 Hz, $CH_2\underline{CH_3}$); 1.88 (6 H, t, *J* 7.5 Hz, $CH_2\underline{CH_3}$); 2.67-2.75 (4 H, q, $\underline{CH_2}CH_3$); 3.56 (6 H, s, CH_3); 3.64 (6 H, s, CH_3); 4.02-4.10 (4 H, q, $\underline{CH_2}CH_3$); 8.34 and 8.41 (2 H, AB quartet, *J* 8.7 Hz, aryl H); 8.55-8.61 (2 H, m, aryl H); 9.96-9.98 (1 H, m, *meso*-15 H); 10.19-10.20 (2 H, m, *meso*-10, 20 H). Mass spectrum (MALDI-TOF) (*m/z*): 599.1 ($M^{+\bullet}$ requires 599.3). (HRMS-ESI Found: $[M + H]^+$ 600.3339. $C_{38}H_{41}N_5O_2$ requires 600.3333; and Found: $[M + Na]^+$ 622.3244. $C_{38}H_{41}N_5NaO_2$ requires 622.3153).

(3) 2,8,13,17-tetraethyl-3,7,12,18-tetramethyl-5-p-amino-phenylporphyrin (H_2AP).

A solution of 2,8,13,17-tetraethyl-3,7,12,18-tetramethyl-5-*p*-nitro-phenylporphyrin (469.0 mg, 0.782 mmol) was dissolved in chloroform (10 mL) and stirred in a

hydrochloric acid/ether mixture (1 M, 40 mL) with tin(II) chloride dihydrate (1.23 g, 5.451 mmol) in the dark for 2 h. The reaction mixture was poured onto ice (50 g) and when the ice melted, chloroform (20 mL) was added. The organic layer was washed with water (200 ml), sodium hydrogencarbonate solution (10%, 200 mL), water (200 mL). The solvent was removed and crude product was purified by column chromatography over silica (dichloromethane/methanol; 100:5). The first purple band was collected and the solvent was removed to give 2,8,13,17-tetraethyl-3,7,12,18-tetramethyl-5-*p*-amino-phenylporphyrin (325.0 mg, 73%) as a purple microcrystalline solid. UV-visible λ_{max} (CH_2Cl_2) (log ε): 310 (4.03), 379 (4.79), 405 (5.15), 503 (4.03), 537 (3.67), 572 (3.67), 625 (3.21) nm. ^{1}H NMR (300 MHz, $CDCl_3$): δ -3.15 (br s, 2 H, inner NH); 1.18 (6 H, t, *J* 7.4 Hz, $CH_2\underline{CH_3}$); 1.88 (6 H, t, *J* 7.5 Hz, $CH_2\underline{CH_3}$); 2.91-2.96 (4 H, q, $\underline{CH_2}CH_3$); 3.57 (6 H, s, CH_3); 3.64 (6 H, s, CH_3); 4.03-4.10 (4 H, q, $\underline{CH_2}CH_3$ overlapped with 2 H, br s, NH_2); 6.99 and 7.03 (2 H, AB quartet, *J* 8.3 Hz, aryl H); 7.86 and 7.93 (2 H, AB quartet, *J* 8.4 Hz, aryl H); 9.91-9.93 (1 H, m, *meso*-15 H); 10.16-10.18 (2 H, m, *meso*-10, 20 H). Mass spectrum (MALDI-TOF) (*m/z*): 569.2 ($M^{+\bullet}$ requires 569.4). (HRMS-ESI Found: $[M + H]^+$ 570.3608. $C_{38}H_{43}N_5$ requires 570.3591).

(4) CoAP.

H_2AP (304.0 mg, 0.534 mmol) and cobalt(II) acetate tetrahydrate (1.0 g, 4.01 mmol) were dissolved in chloroform (30 mL) and methanol (15 mL), which was heated at reflux for 20 min. The solvent was removed and the crude product was dissolved in dichloromethane (100 mL) and washed with water (3 × 200 mL). The solvent was then removed to give CoAP (328.0 mg, 98%) as a red microcrystalline solid. UV-visible λ_{max} (CH_2Cl_2) (log ε): 330 (4.06), 398 (4.85), 423sh (4.35), 525 (3.82), 557 (3.90) nm. Mass spectrum (MALDI-TOF) (*m/z*): 626.0 ($M^{+\bullet}$ requires 626.3). (HRMS-ESI Found: $[M]^+$ 626.2714. $C_{38}H_{41}CoN_5$ requires 626.2689).

2. Electrochemistry of CoAP

Electrochemical measurements of H_2AP and CoAP were performed on a potentiostat (PGSTAT 30, Eco-Chemie, Netherlands) in a three-electrode configuration, using a 3 mm-in-diameter Pt electrode, a Pt wire and a Ag wire as the working, counter and quasi-reference electrode, respectively. The concentration of H_2AP and CoAP is 1 mM. The supporting electrolyte used was tetrabutylammonium hexafluorophosphate ($TBAPF_6$, ≥ 99%) in 0.1 M. The solution was bubbled by nitrogen before measurements. The potential scale was calibrated to the normal hydrogen electrode by using ferrocene as the internal reference ($E^{o}_{Fc^+/Fc}$ = 0.64 V) [4].

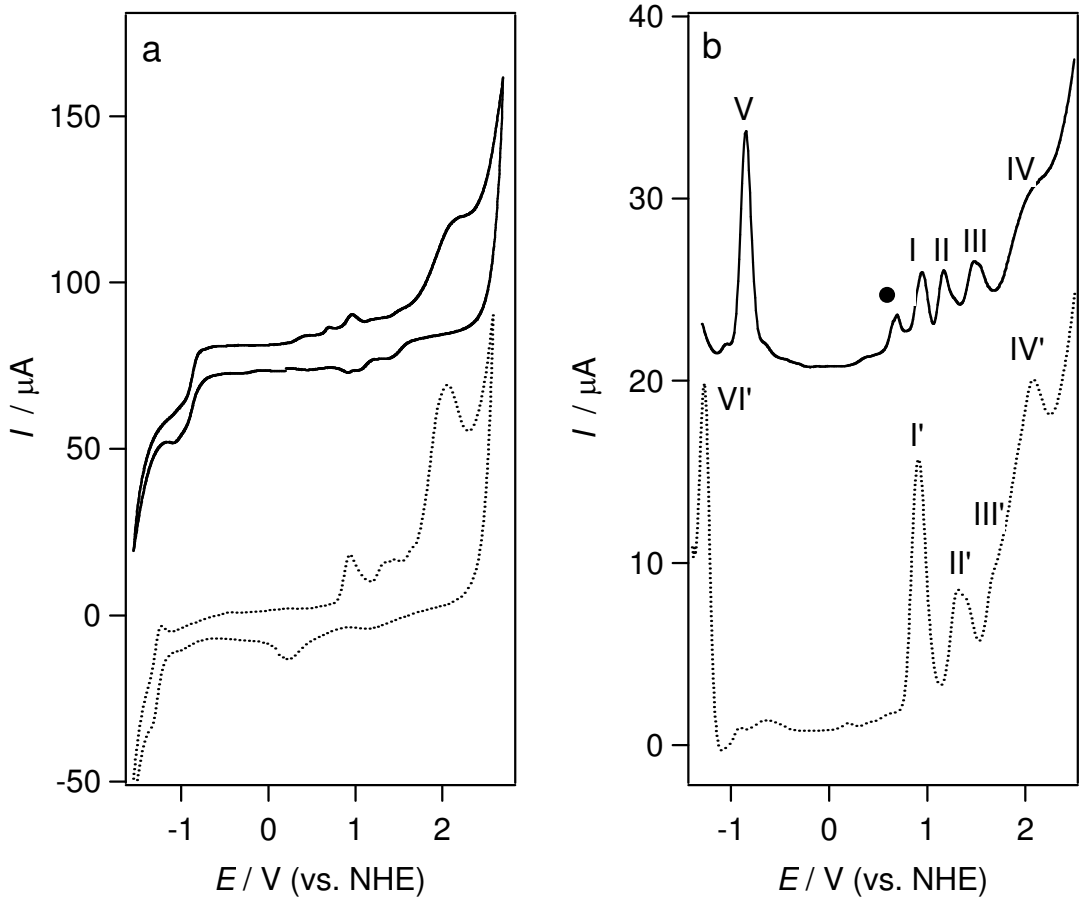

Figure S-1. Cyclic voltammograms at a scan rate of 0.1 V s^{-1} (a) and square wave voltammgrams with a frequency 8 Hz, potential step 0.01 V and potential amplitude 0.02 V (b): CoAP (full line) and H_2AP (dotted line).

Comparing the voltammetric responses of CoAP with those of H_2AP, as shown in Figure S-1b, the waves at 0.69 V and –0.85 (labelled by a black dot and V, respectively) are assigned to the first oxidation and reduction of cobalt centre, namely, $Co^{III}AP^+/Co^{II}AP$ and $Co^{II}AP/Co^{I}AP^-$ couples. Other waves, such as labelled by I, II, III and IV, and correspondingly I', II', III' and IV' for H_2AP can be assigned to the first ring oxidation, the second ring oxidation, amine oxidation and electro-polymerization, respectively. The wave VI' can be ascribed to the first ring reduction.

3. Derivation of Surface Excess Concentration of CoAP

At constant temperature and pressure, the interfacial Gibbs adsorption equation involving adsorption of CoAP and protonated CoAP, denoted as, B and BH^+, can be expressed as follows [4]:

$$\begin{aligned} -\mathrm{d}\gamma_{\mathrm{T,P}} &= \sum_i \Gamma_i \mathrm{d}\mu_{\mathrm{i}} \\ &= \Gamma_{\mathrm{H_2O}}\mathrm{d}\mu_{\mathrm{H_2O}} + \Gamma_{\mathrm{Li^+}}\mathrm{d}\mu_{\mathrm{Li^+}} + \Gamma_{\mathrm{H^+}}\mathrm{d}\mu_{\mathrm{H^+}} + \Gamma_{\mathrm{Cl^-}}\mathrm{d}\mu_{\mathrm{Cl^-}} + \Gamma_{\mathrm{DCE}}\mathrm{d}\mu_{\mathrm{DCE}} \\ &\quad + \Gamma_{\mathrm{B}}\mathrm{d}\mu_{\mathrm{B}} + \Gamma_{\mathrm{BO_2}}\mathrm{d}\mu_{\mathrm{BO_2}} + \Gamma_{\mathrm{BO_2H^+}}\mathrm{d}\mu_{\mathrm{BO_2H^+}} + \Gamma_{\mathrm{BA^+}}\mathrm{d}\mu_{\mathrm{BA^+}} + \Gamma_{\mathrm{TB^-}}\mathrm{d}\mu_{\mathrm{TB^-}} \end{aligned} \quad \text{(S-1)}$$

where γ is the surface tension and Γ represents the surface excess concentration, respectively. The subscripts, B, BO_2 and BO_2H^+, represent CoAP, $(Co\text{-}O_2)AP$ and $[(Co\text{-}O_2H)AP]^+$, respectively. The electrochemical potential terms in eq. S-1 are subject to the following relationships:

$$\begin{aligned} \mathrm{d}\mu_{\mathrm{LiCl}} &= \mathrm{d}\mu_{\mathrm{Li^+}} + \mathrm{d}\mu_{\mathrm{Cl^-}} \\ \mathrm{d}\mu_{\mathrm{HCl}} &= \mathrm{d}\mu_{\mathrm{H^+}} + \mathrm{d}\mu_{\mathrm{Cl^-}} \\ \mathrm{d}\mu_{\mathrm{BATB}} &= \mathrm{d}\mu_{\mathrm{BA^+}} + \mathrm{d}\mu_{\mathrm{TB^-}} \\ \mathrm{d}\mu_{\mathrm{BO_2}} &= \mathrm{d}\mu_{\mathrm{B}} + \mathrm{d}\mu_{\mathrm{O_2}} \\ \mathrm{d}\mu_{\mathrm{BO_2H^+}} &= \mathrm{d}\mu_{\mathrm{B}} + \mathrm{d}\mu_{\mathrm{O_2}} + \mathrm{d}\mu_{\mathrm{H^+}} \end{aligned} \quad \text{(S-2)}$$

And eq. S-1 can be rewritten as:

$$\begin{aligned} -\mathrm{d}\gamma_{\mathrm{T,P}} &= \Gamma_{\mathrm{H_2O}}\mathrm{d}\mu_{\mathrm{H_2O}} + \Gamma_{\mathrm{Li^+}}\mathrm{d}\mu_{\mathrm{LiCl}} + \left(\Gamma_{\mathrm{H^+}} + \Gamma_{\mathrm{BO_2H^+}}\right)\mathrm{d}\mu_{\mathrm{HCl}} - \left(\Gamma_{\mathrm{Li^+}} + \Gamma_{\mathrm{H^+}} + \Gamma_{\mathrm{BO_2H^+}} - \Gamma_{\mathrm{Cl^-}}\right)\mathrm{d}\mu_{\mathrm{Cl^-}} \\ &\quad + \left(\Gamma_{\mathrm{B}} + \Gamma_{\mathrm{BO_2}} + \Gamma_{\mathrm{BO_2H^+}}\right)\mathrm{d}\mu_{\mathrm{B}} + \left(\Gamma_{\mathrm{BO_2}} + \Gamma_{\mathrm{BO_2H^+}}\right)\mathrm{d}\mu_{\mathrm{O_2}} \\ &\quad + \Gamma_{\mathrm{DCE}}\mathrm{d}\mu_{\mathrm{DCE}} + \Gamma_{\mathrm{BA^+}}\mathrm{d}\mu_{\mathrm{BATB}} - \left(\Gamma_{\mathrm{BA^+}} - \Gamma_{\mathrm{TB^-}}\right)\mathrm{d}\mu_{\mathrm{TB^-}} \end{aligned} \quad \text{(S-3)}$$

The charge densities in each phases and the electroneutrality condition give:

$$\sigma = \left(\Gamma_{Li^+} + \Gamma_{H^+} + \Gamma_{BO_2H^+} - \Gamma_{Cl^-}\right)F$$
$$\sigma = -\left(\Gamma_{BA^+} - \Gamma_{TB^-}\right)F \qquad \text{(S-4)}$$

Thus, eq. S-1 can be reorganized to be:

$$-\mathrm{d}\gamma_{T,P} = \frac{\sigma}{F}\left(\mathrm{d}\tilde{\mu}_{TPFB^-} - \mathrm{d}\tilde{\mu}_{Cl^-}\right) + \Gamma_{H_2O}\mathrm{d}\mu_{H_2O} + \Gamma_{Li^+}\mathrm{d}\mu_{LiCl} + \left(\Gamma_{H^+} + \Gamma_{BO_2H^+}\right)\mathrm{d}\mu_{HCl}$$
$$+\left(\Gamma_B + \Gamma_{BO_2} + \Gamma_{BO_2H^+}\right)\mathrm{d}\mu_B + \left(\Gamma_{BO_2} + \Gamma_{BO_2H^+}\right)\mathrm{d}\mu_{O_2} + \Gamma_{DCE}\mathrm{d}\mu_{DCE} + \Gamma_{BA^+}\mathrm{d}\mu_{BATB} \qquad \text{(S-5)}$$

The first term is associated with the voltage imposed between two terminals of the electrochemical cell, which can be further related to the Galvani potential difference across the interface:

$$\left(\mathrm{d}\tilde{\mu}_{TPFB^-} - \mathrm{d}\tilde{\mu}_{Cl^-}\right) = F\mathrm{d}\Delta_o^w\phi \qquad \text{(S-6)}$$

Introducing eq. S-6 to S-5 yields:

$$-\mathrm{d}\gamma_{T,P} = \sigma\mathrm{d}\Delta_o^w\phi + \Gamma_{H_2O}\mathrm{d}\mu_{H_2O} + \Gamma_{Li^+}\mathrm{d}\mu_{LiCl} + \left(\Gamma_{H^+} + \Gamma_{BO_2H^+}\right)\mathrm{d}\mu_{HCl}$$
$$+\left(\Gamma_B + \Gamma_{BO_2} + \Gamma_{BO_2H^+}\right)\mathrm{d}\mu_B + \left(\Gamma_{BO_2} + \Gamma_{BO_2H^+}\right)\mathrm{d}\mu_{O_2} + \Gamma_{DCE}\mathrm{d}\mu_{DCE} + \Gamma_{BA^+}\mathrm{d}\mu_{BATB} \qquad \text{(S-7)}$$

Thus, the surface excess concentration of CoAP species ($\Gamma_B + \Gamma_{BO_2} + \Gamma_{BO_2H^+}$), as described by eq. 5 in the paper, can be derived from eq. S-7.

4. Titration of CoAP with TFA

Spectra of titrating 25 μM CoAP with TFA (Figure S-2, a and b) show that the protonation of CoAP occurs in two steps with a transition stage. The first step shows that the Soret band at 423 nm increases at the cost of the original one at 397 nm, as well as the appearance of a new band at 356 nm, with increasing the concentration of TFA. This is

assigned to be the proton facilitation on the oxygenation of cobalt centre, by the formation of hydroperoxyl radical.

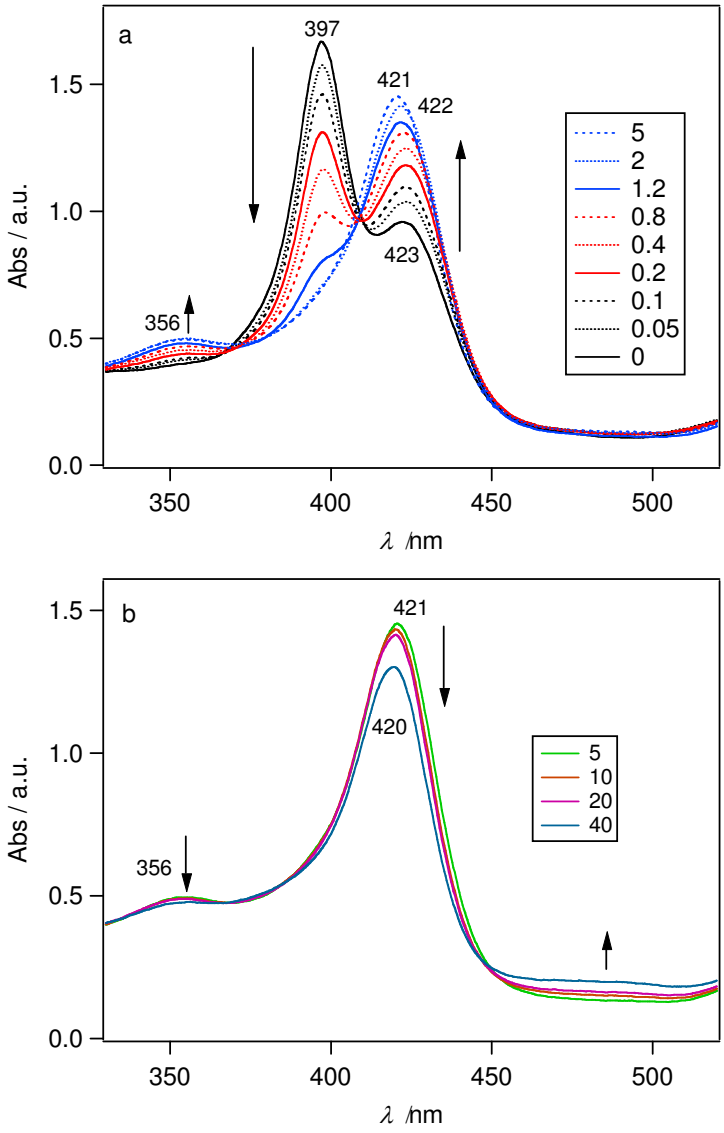

Figure S-2. Spectrophotometric titration of CoAP with TFA.

When the TFA concentration is between 1 mM and 5 mM, the titration reaches the transition stage. The Soret band at 423 starts shifting to the left, for examples 422 nm at 1.2 mM and 421 nm at 5 mM, but the second Soret band and the band at 356 nm keep increasing and the first one keeps decreasing and finally is completely damped at 5 mM.

When the TFA concentration is higher than 5 mM, both the second Soret band and the band at 356 nm start decreasing, with the appearance of a very broad, flat absorption around 480 nm. This is due to the protonation of the peripheral amine. As the TFA concentration is above 20 mM, the second Soret band resides at 420 nm, which does not shift but decrease in intensity with the TFA concentration.

5. Comparison with CoP and CoOEP

The catalysis of CoAP on oxygen reduction by Fc was compared with two other compounds, cobalt porphine (CoP) and 2,3,7,8,12,13,17,18-octaethylporphyrin cobalt(II) (CoOEP), which are not amphiphilic. As shown in Figure S-3a, the catalytic ability of CoAP is apparently much more efficient than CoP and CoOEP (more clearly can be seen in the logarithmic scale, Figure S-3b). In particular, the comparison with CoOEP highlights the role of the amphiphilicity of the catalyst as both CoAP and CoOEP have the same redox potential for the first oxidation (0.69 V *vs* SHE), whereas CoP is more difficult to oxidize (1.15 V *vs* SHE) [5].

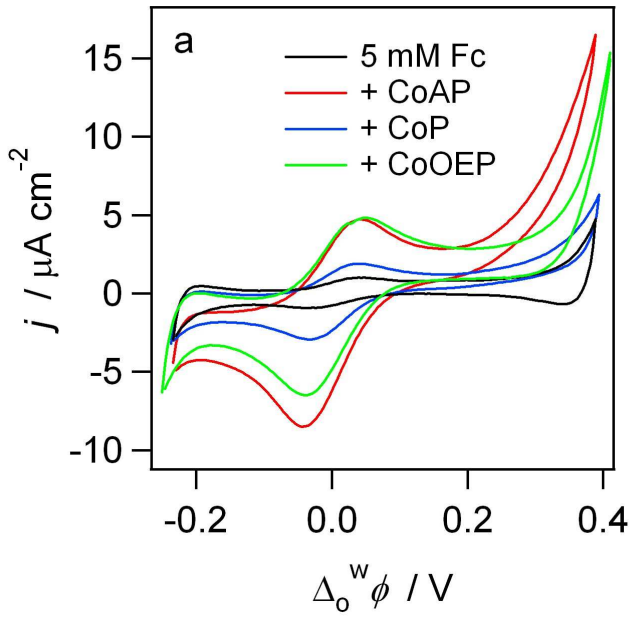

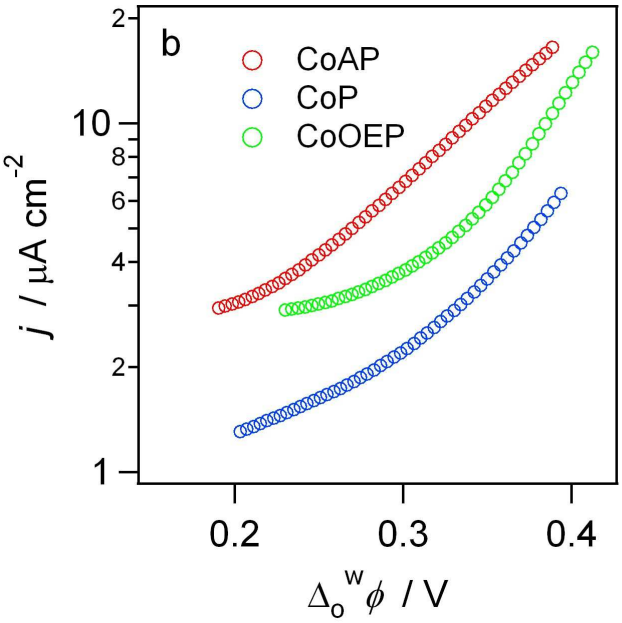

Figure S-3. (a) Comparison of CVs in the presence of different cobalt porphyrins: 25 μM CoAP (red), 25 μM CoP (blue) and 50 μM CoOEP (green) and 5 mM Fc. The black curve represents the case of 5 mM Fc alone. Cell 1 was used as shown in the manuscript, pH = 2, scan rate 0.05 V s^{-1}. (b) Logarithmic plots of the catalytic currents in a: CoAP (red), CoP (blue) and CoOEP (green).

References:

[1] Tanaka, M.; Ohkubo, K.; Gros, C. P.; Guilard, R.; Fukuzumi, S. *J. Am. Chem. Soc.* **2006**, *128*, 14625-14633.

[2] Barton, D. H. R.; Zard, S. Z. *J. Chem. Soc., Chem. Commun.* **1985**, 1098-100.

[3] Barton, D. H. R.; Kervagoret, J.; Zard, S. Z. *Tetrahedron* **1990**, *46*, 7587-98.

[4] Eugster, N.; Fermin, D. J.; Girault, H. H. *J. Phys. Chem. B* **2002**, *106*, 3428-3433.

[5] Partovi-Nia, R. Ph. D Thesis: Electrocatalysis at liquid|liquid interfaces, EPFL no.4260, Lausanne, 2010.